fermentation

MDPI

Article

Isolation, Characterization, and Genomic Elucidation of HRY1: An Unconventional but Highly Efficient Phosphate-Solubilizing *Escherichia coli*

Ruiyan He, Sa Zhang and Yuanwang Liu *

State Key Laboratory of Metastable Materials Science and Technology, Hebei Key Laboratory of Heavy Metal Deep-Remediation in Water and Resource Reuse, School of Environmental and Chemical Engineering, Yanshan University, Qinhuangdao 066004, China; hry_04@163.com (R.H.)

* Correspondence: liuyuanwang@ysu.edu.cn

Abstract

Phosphate-solubilizing bacteria (PSB) are pivotal in the cycling of phosphorus within terrestrial ecosystems and hold great promise for sustainable agriculture. In this study, we report the isolation of HRY1—a highly efficient phosphate-solubilizing strain—identified as *Escherichia coli*, a bacterium not traditionally recognized for plant-beneficial traits. Under optimized conditions (glucose as carbon source, $(NH_4)_2SO_4$ as nitrogen source, pH 7.0, 1% inoculum, and 5 g/L $Ca_3(PO_4)_2$), HRY1 consistently solubilized ~16% of inorganic phosphorus, with peak activity coinciding with its stationary growth phase (14 h). Whole-genome sequencing revealed a comprehensive genetic toolkit for phosphorus mobilization, including eight genes implicated in organic acid-mediated mineral dissolution, five high-affinity phosphate transporter genes (*pit* and *pst* gene cluster), and three two-component regulatory systems responsive to phosphate starvation (e.g., *pho*BR). The functional integration of these systems suggests a multifaceted strategy combining acidification, active uptake, and adaptive regulation to thrive under phosphorus limitation. Our findings redefine the ecological scope of *E. coli* and uncover an unconventional yet potent PSB candidate with significant potential for biofertilizer development and soil phosphorus activation. This discovery reveals *E. coli*'s untapped potential for phosphorus solubilization, with HRY1's novelty residing in its high efficiency under optimized conditions and its practical promise as a biofertilizer.

Keywords: phosphate-solubilizing bacteria; Identification; phosphate-solubilizing properties; whole-genome sequencing

Check for updates

Academic Editor: Pierre Christen

Received: 5 January 2026
Revised: 3 February 2026
Accepted: 12 February 2026
Published: 15 February 2026

Copyright: © 2026 by the authors. Licensee MDPI, Basel, Switzerland. This article is an open access article distributed under the terms and conditions of the Creative Commons Attribution (CC BY) license.

1. Introduction

Phosphorus is an essential nutrient for plant growth and development, extensively involved in numerous critical metabolic processes such as photosynthesis, energy transfer, signal transduction, respiration, and biological nitrogen fixation [1]. Although total soil phosphorus content is typically approximately 0.05%, the majority exists in insoluble inorganic forms (e.g., calcium, iron, or aluminum phosphates) or stable organic complexes [2]. Consequently, the fraction of plant-available phosphorus is extremely limited, generally accounting for less than 0.1% of the total phosphorus pool due to rapid fixation and inherently low solubility in most soils [3]. In contemporary agricultural systems, the intensive application of phosphate fertilizers has become a widespread practice to meet crop phosphorus demands. Nevertheless, the actual phosphorus utilization efficiency by crops remains

substantially low, with values ranging from 11.5% to 13.4% [4]. This inefficiency results in substantial accumulation of phosphorus in unavailable forms within soil profiles, consequently constraining agricultural productivity. Such inefficient phosphorus use not only perpetuates a state of "phosphorus hunger" in crops but also raises serious environmental concerns, including soil acidification and eutrophication of aquatic ecosystems [5]. Consequently, developing innovative strategies to effectively mobilize the native soil phosphorus pool and enhance phosphorus bioavailability has emerged as a critical scientific challenge scientific priority to advance sustainable agriculture.

Phosphate-solubilizing bacteria (PSB) are functional microorganisms capable of converting insoluble phosphorus into plant-available forms through multiple biochemical mechanisms, playing a crucial role in regulating the transformation of soil phosphorus speciation [6]. The phosphorus-solubilizing mechanisms primarily involve acidification, enzymatic hydrolysis, respiratory metabolism, and NH_4^+ assimilation processes [7]. Notably, PSB not only mobilize insoluble phosphorus in soils but also effectively prevent the re-fixation of solubilized phosphorus through chelation, thereby maintaining phosphorus bioavailability. Currently, PSB-based microbial fertilizers have been widely adopted in agricultural production, with empirical evidence demonstrating their significant contributions to promoting crop growth, improving yield, and reducing both chemical phosphorus fertilizer application and environmental impacts [8]. Consequently, the development of PSB-based bio-phosphate fertilizers for partial substitution of chemical phosphorus fertilizers has emerged as a viable strategy to advance the green transformation of agriculture, holding considerable promise for future eco-agricultural systems. Despite these advances, the majority of characterized PSB belong to canonical genera such as *Pseudomonas*, *Bacillus*, and *Burkholderia*, and there remains a paucity of reports on highly efficient phosphate solubilizers from unconventional or underexplored taxonomic lineages [9]. Moreover, the genetic basis underlying phosphorus solubilization in non-model or atypical PSB is often poorly characterized, limiting their rational design and deployment in biofertilizer design.

This study collected soil samples and screened for a highly efficient phosphorus-solubilizing bacterium, *Escherichia coli* HRY1, through selective isolation and cultivation. Single-factor optimization methods were systematically employed to investigate optimal phosphorus-solubilizing conditions and characterize the strain's solubilization properties. Furthermore, whole-genome sequencing was utilized to obtain the complete genomic information of this strain, enabling in-depth analysis of its phosphorus-solubilizing-related functional genes. This work aims to provide novel microbial resources and theoretical foundations for the development and application of highly efficient phosphorus-solubilizing bacterial agents.

2. Materials and Methods

2.1. Soil Sample Collection

Soil samples were collected in November 2024 from the campus of Yanshan University (39° N, 119° E), Qinhuangdao City, China. Approximately 5 g of topsoil (0–10 cm depth) was collected from five points in the campus. The soil samples from all points were thoroughly homogenized to form a composite sample, placed in a sterile sealed bag, immediately transported to the laboratory under low-temperature conditions in an icebox, and stored at 4 °C for further use.

2.2. Isolation and Screening of Bacterial Strains

Inorganic PSB were isolated using National Botanical Research Institute's phosphate (NBRIP) agar medium, which contained the following ingredients L^{-1}: glucose, 10 g; $(NH_4)_2SO_4$, 0.1 g; KCl, 0.2 g; $MgSO_4 \cdot 7H_2O$, 0.25 g; $MgCl_2$, 5.0 g; $Ca_3(PO_4)_2$, 5.0 g; and agar,

18.0. Specifically, 1 g of soil sample was inoculated into 100 mL of LB liquid medium, which contained L^{-1}: peptone, 10 g; yeast extract, 5 g; and NaCl, 10 g, and incubated at 30 °C with shaking at 150 rpm for 48 h (all chemicals used in the experiment were purchased from Kemiou Chemical Reagent Co., Ltd., Tianjin, China). The resulting culture was then subjected to serial dilution. Aliquots of 100 µL from dilution gradients of 10^{-1}, 10^{-3}, 10^{-5}, 10^{-7}, 10^{-8}, and 10^{-9} were spread onto sterile NBRIP agar plates. The plates were incubated upside down at 30 °C for 72 h. Colonies exhibiting clear phosphate-solubilizing halos were selected and purified by repeated streaking on LB agar. Purified isolates were subsequently re-streaked onto NBRIP agar to confirm their phosphate-solubilizing activity based on halo formation. Strains demonstrating consistent and robust solubilization capacity across biological replicates were retained for further characterization.

2.3. Microbiological Identification of Bacterial Strains

2.3.1. Morphological Characteristics

A single colony of the PSB was streaked onto LB agar and incubated at 30 °C for 48 h. Colony morphology—including shape, color, margin, and elevation—was observed and recorded. For Gram staining, cells were harvested from an LB broth culture during the logarithmic growth phase, stained using the standard Gram protocol, and examined under a light microscope to determine cellular morphology and Gram reaction.

2.3.2. 16S rRNA Gene Sequencing

Genomic DNA was extracted from cells of the PSB grown in LB liquid medium using the MiniBEST Universal Genomic DNA Extraction Kit Ver.5.0 (TaKaRa, Kusatsu, Japan) following the manufacturer's instructions. The extracted DNA was used as the template for PCR amplification of the 16S rRNA gene with universal primers 27F/1492R. Amplification products were separated by electrophoresis on a 1.0% (*w*/*v*) agarose gel, and target bands were excised and purified using a commercial gel extraction kit. The purified amplicons were subsequently sent to SinoGenoMax Co., Ltd. (Beijing, China) for sequencing. The obtained sequences were trimmed and assembled, then subjected to BLASTn analysis against the National Center for Biotechnology Information (NCBI) nucleotide database. Reference sequences of closely related type strains (with ≥99% sequence similarity) were selected and a phylogenetic tree was constructed using the Neighbor-Joining method in MEGA (version 5.0, Mega Limited, Auckland, New Zealand), with bootstrap support calculated from 1000 replicates, to infer the taxonomic affiliation of the isolate.

2.4. Determination of Growth Curve

A single colony of strain HRY1 was aseptically inoculated into 100 mL of LB broth and incubated at 30 °C with shaking at 150 rpm for 24 h to obtain a pre-culture. Cells were harvested by centrifugation at 8000 rpm for 5 min at 4 °C, washed twice with sterile distilled water to remove residual medium, and resuspended in the same volume of sterile water. The optical density of the resulting suspension was adjusted to OD_{600} = 1.0 using a UV–Vis spectrophotometer (TianGuang Optical Instruments Co., Ltd., Tianjin, China). For growth curve determination, this standardized suspension was inoculated at 1% (*v*/*v*) into fresh 100 mL LB broth (uninoculated medium served as blank control) and incubated at 30 °C with shaking at 180 rpm for 72 h. Samples were collected at regular intervals, and OD_{600} values were measured to monitor cell density over time, enabling identification of the characteristic growth phases: lag phase, logarithmic phase, stationary phase, and decline phase.

2.5. Optimization of Phosphate-Solubilizing Conditions

The phosphate-solubilizing activity of strain HRY1 was evaluated in NBRIP liquid medium using single-factor optimization method. In this approach, each of the following variables—carbon source, nitrogen source, initial pH, inoculum size, and $Ca_3(PO_4)_2$ concentration—was systematically varied, while all other parameters were held constant. Specifically:

(1) Carbon source: glucose, soluble starch, and sucrose were tested individually at 10 g L^{-1};
(2) Nitrogen source: $(NH_4)_2SO_4$ (control), NH_4Cl, urea, and KNO_3 were supplied at 0.1 g L^{-1};
(3) Initial pH: adjusted to 5.0, 6.0, 7.0, 8.0, or 9.0 using 1 M HCl or NaOH;
(4) Inoculum size: 1%, 2%, 4%, or 8% (v/v) of a standardized suspension (OD_{600} = 1.0);
(5) $Ca_3(PO_4)_2$ concentration: Set at 2.5, 5.0, or 15.0 g L^{-1}.

All experimental groups were established with corresponding uninoculated media as blank controls, and each treatment was performed in triplicate. With the exception of the inoculum size optimization experiment, all other groups were inoculated with 1% (v/v) bacterial suspension. After a specified incubation period, samples were collected and centrifuged at 8000 rpm for 10 min. The soluble phosphorus content in the supernatant was determined using molybdenum–antimony anti spectrophotometric method (expressed as PO_4^{3-}, unit: mg L^{-1}). Phosphate solubilization efficiency (%) was calculated as:

$$\text{Phosphate Solubilization Efficiency (\%)} = ((C_{nm} - C_{n0}) - (C_{nm0} - C_{n00}))/P_{total} \times 100\% \quad (1)$$

where n is the treatment number, m is the number of cultivation days; C_{nm} and C_{n0} represent the soluble phosphorus concentrations (mg L^{-1}) of treatment n on day m and initially, respectively; C_{nm0} and C_{n00} represent the soluble phosphorus concentrations (mg L^{-1}) of the blank control (corresponding to treatment n) on day m and initially, respectively; P_{total} represents total added phosphorus concentration (mg P L^{-1}).

In addition, it should be noted that the approach above evaluates factors individually and does not account for potential interaction effects between variables. Therefore, the resulting conditions represent the best combination identified within the tested ranges under the single-factor optimization method, rather than a statistically validated global optimum.

2.6. Whole-Genome Sequencing

Strain HRY1 was cultured in LB medium at 30 °C with shaking and 150 rpm for 24 h. Cells were harvested by centrifugation at 8000 rpm for 10 min at 4 °C. The supernatant was discarded, and the cell pellet was washed three times with sterile distilled water. The washed cells were rapidly frozen in liquid nitrogen and stored at −80 °C. Genomic DNA was extracted and sent to Wuhan Frasergen Bioinformatics Co., Ltd. (Wuhan, China) for whole-genome sequencing. A complete, circularized genome was generated using single-molecule real-time (SMRT) sequencing on the PacBio Revio platform. Raw reads were assembled de novo into a single contig using Flye (v2.9). Protein-coding genes were predicted using Glimmer (v3.02), tRNA genes with tRNAscan-SE (v2.0.9), and rRNA operons with RNAmmer (v1.2). Functional annotation was performed by aligning the predicted protein sequences against the NCBI Non-Redundant Protein (NR) and Kyoto Encyclopedia of Genes and Genomes (KEGG) databases. A circular genome visualization was constructed using shinyCircos (v2.0) [10]. Special attention was given to genes associated with organic acid biosynthesis and phosphorus metabolism to elucidate the molecular basis underlying the strain's phosphate-solubilizing capability.

2.7. Statistical Analysis

Following standard data processing methods for environmental microbiology research, data were organized and analyzed the data using Microsoft Excel 2024 (Microsoft Corporation, Redmond, WA, USA). Phylogenetic trees illustrating the taxonomic placement of strain HRY1 were constructed using MEGA 11 (Mega Limited, Auckland, New Zealand). Visualization of strain growth curves and phosphate solubilization efficiency variations under different conditions was performed using Origin 2024 (OriginLab, Inc., Northampton, MA, USA). The circular genome map for the strain was performed using Circos (v0.69-9). Taxonomic classification based on NR database annotation was visualized using Python (v3.10). KEGG annotation taxonomic classification map was rendered using the R (v4.3.0) package Pathview. The gene cluster structure of inorganic phosphate solubilization genes was illustrated with SnapGene Viewer 8.0 (GSL BIOTECH, LLC, New York, NY, USA).

3. Results

3.1. Screening and Identification of Phosphate-Solubilizing Bacteria

Two phosphate-solubilizing bacterial strains, designated HRY1 and HRY2, were isolated from soil based on their ability to form clear halos on NBRIP agar plates. After 48 h of incubation, both strains produced distinct solubilization halos, with HRY1 exhibiting a markedly larger halo diameter compared to HRY2 (Figure 1). This phenotypic difference suggested superior phosphate-solubilizing activity of HRY1, which was therefore selected for further characterization.

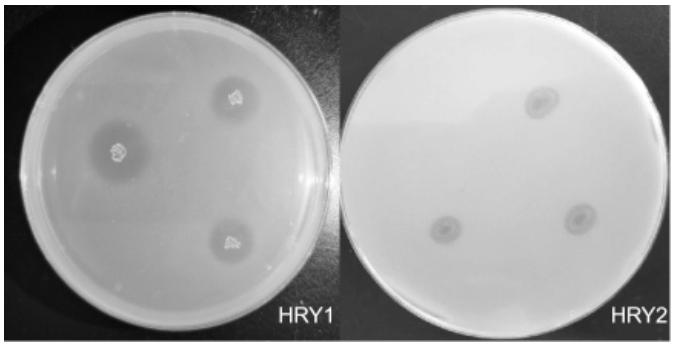


Figure 1. Phosphate-solubilizing effects of the two isolated bacterial strains.

The typical colonial morphology of strain HRY1 on agar plates is shown in Figure 2a. It formed circular, light-yellow colonies on LB agar after 48 h of incubation at 30 °C, with convex elevation, entire margins, and a diameter of approximately 1 mm. Colonies were translucent with a smooth, homogeneous surface. Gram staining showed red-stained rod-shaped cells under light microscopy (Figure 2b), confirming that HRY1 is a Gram-negative bacterium.

The 16S rRNA gene of strain HRY1 was amplified by PCR and sequenced by SinoGenoMax Co., Ltd. (Beijing, China). BLASTn analysis against the NCBI database revealed 99.8% sequence identity with multiple *E. coli* strains. To further assess its phylogenetic affiliation, a neighbor-joining tree was constructed using 16S rRNA gene sequences of closely related type strains. As shown in Figure 2c, HRY1 clustered within a well-supported clade together with reference *E. coli* strains, including *E. coli* CBE Ec-1, W99, and FBC1018. These results strongly support the classification of strain HRY1 as *E. coli*.

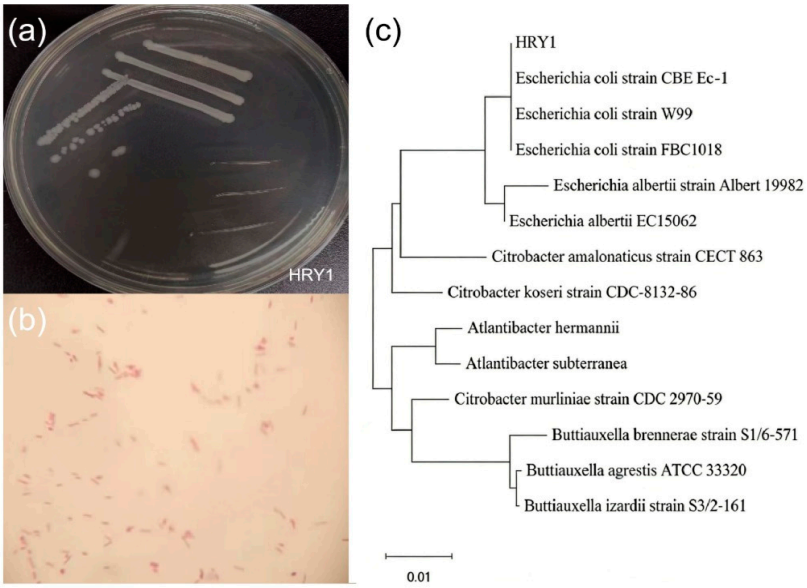


Figure 2. Strain identification chart of strain HRY1. (**a**) Colonial morphology; (**b**) Gram staining characterization; (**c**) Phylogenetic tree of HRY1 based on 16S rRNA gene sequence.

3.2. Bacterial Growth Curve

The growth curve of strain HRY1 is presented in Figure 3. The strain exhibited a lag phase from 0 to 4 h, characterized by slow proliferation. It entered the logarithmic growth phase between 5 and 13 h, demonstrating a significantly increased growth rate and rapid biomass accumulation. During the period of 14–48 h, the strain reached the stationary phase, during which biomass continued to accumulate but at a progressively declining growth rate. Beyond 48 h, the total viable cell count declined, marking the onset of the death (decline) phase. Based on these growth characteristics, the cells harvested at 8 h—corresponding to the mid-logarithmic phase when metabolic activity and proliferation rate are maximal—were selected as the inoculum for subsequent experiments to ensure uniform physiological state and optimal growth performance.

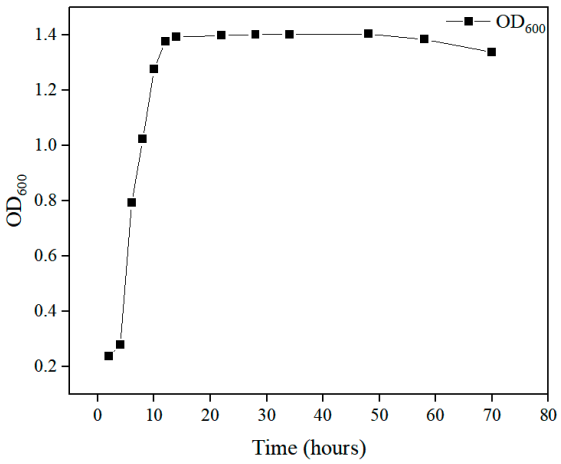


Figure 3. Growth curve of strain HRY1.

3.3. Optimization of Phosphate-Solubilizing Conditions

The phosphate solubilization efficiency of strain HRY1 under different carbon source conditions is shown in Figure 4a. The phosphate solubilization efficiency was monitored at 24-h intervals over a 7-day incubation period. The results demonstrated that the strain exhibited the strongest phosphate-solubilizing capacity when glucose was used as the carbon

source, achieving a maximum solubilization efficiency of 17.62%, with a corresponding soluble phosphorus concentration of 196.90 mg L^{-1}—higher than that observed with soluble starch (3.58%, 54.68 mg L^{-1}) or sucrose (2.72%, 49.02 mg L^{-1}) (Table S1). Among the carbon sources tested, the glucose group maintained consistently high performance throughout the incubation. The sucrose group showed an initial decline followed by a gradual increase in phosphate solubilization. In contrast, soluble starch yielded the lowest solubilization efficiency, likely because its complex polymeric structure requires extracellular hydrolysis prior to cellular uptake and metabolism. Although a slight decline was observed in the glucose group during the later stages of cultivation, possibly due to saturation of bacterial growth, its overall phosphate solubilization efficiency remained significantly superior to other carbon sources. Collectively, these results indicate that glucose is the optimal carbon source for promoting phosphate solubilization by strain HRY1.

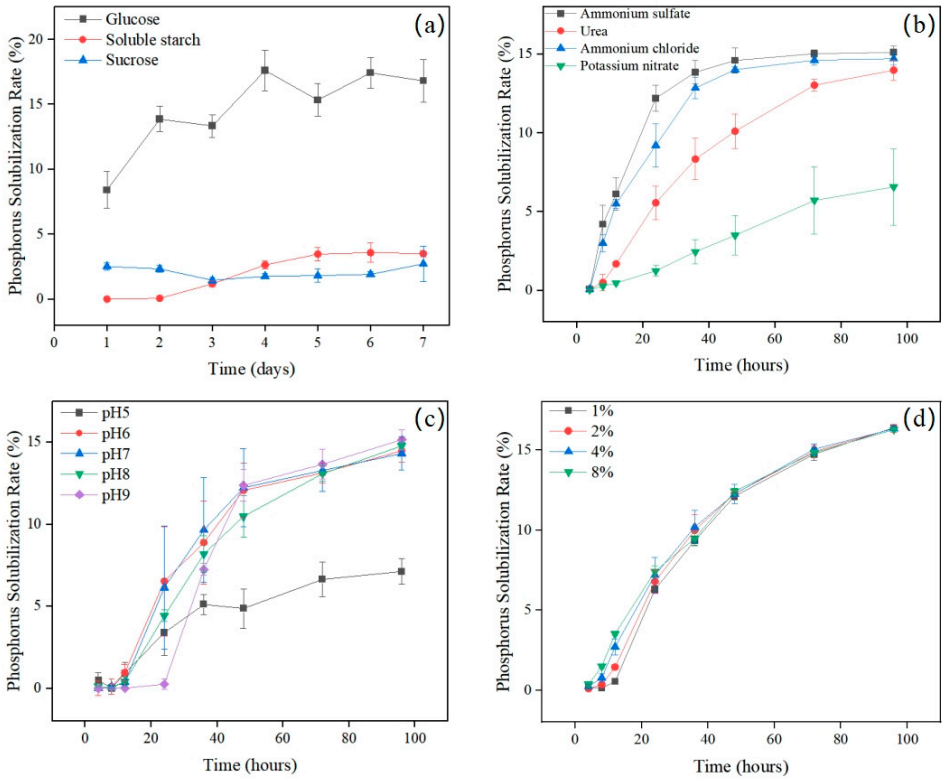


Figure 4. Effects of different culture conditions on the phosphate-solubilizing capacity of strain HRY1. (**a**) Carbon source; (**b**) Nitrogen source; (**c**) pH; (**d**) Inoculum size.

Based on the carbon source optimization results, the phosphate solubilization efficiencies of strain HRY1 across all treatment groups remained essentially unchanged after 96 h of incubation. Therefore, a 96-h period was adopted as the standard duration for subsequent optimization experiments. Sampling was conducted at 4, 8, 12, 24, 36, 48, 72, and 96 h to determine phosphorus concentration and calculate the corresponding phosphate solubilization efficiencies.

After the identification of glucose as the optimal carbon source, further optimization of nitrogen sources was conducted, with results shown in Figure 4b and Table S2. Among the tested nitrogen sources, ammonium sulfate yielded the highest phosphate solubilization efficiency, reaching a maximum of 15.10%, which corresponds to a soluble phosphorus concentration of 166.23 mg L^{-1}—superior to ammonium chloride (14.70%, 157.56 mg L^{-1}), urea (13.97%, 152.74 mg L^{-1}), and potassium nitrate (6.56%, 78.21 mg L^{-1}). In both the ammonium sulfate and ammonium chloride treatments, phosphate solubilization increased

rapidly during the early cultivation stage, synchronizing with the vigorous growth of the strain in the early exponential phase, indicating that readily available ammonium salts can promptly support phosphate-solubilizing metabolism. Although the ammonium chloride group showed a similar kinetic profile, its overall efficiency was lower. The urea group demonstrated weak solubilization capacity during the early cultivation stage, which gradually increased later, reflecting the need for hydrolysis and conversion before efficient utilization. In contrast, the potassium nitrate group consistently yielded the lowest solubilization efficiency, with its solubilization curve increasing slowly throughout the incubation, demonstrating that the energy-consuming assimilation pathway severely impedes the growth-coupled phosphate solubilization process. These results indicate that ammonium sulfate is the optimal nitrogen source for efficient phosphate solubilization by strain HRY1.

Building upon the established optimal conditions of glucose as carbon source and ammonium sulfate as nitrogen source, further optimization of initial pH was conducted, with results presented in Figure 4c. Within the pH range of 5.0–9.0, the phosphorus solubilization efficiencies of strain HRY1 at 96 h were 7.13% (pH 5.0), 14.48% (pH 6.0), 14.31% (pH 7.0), 14.78% (pH 8.0), and 15.16% (pH 9.0). Notably, under acidic conditions (pH 5.0), the phosphorus solubilization efficiency was relatively high as early as 4 h, with a corresponding soluble phosphorus concentration of 128.25 mg L^{-1}, likely attributed to the non-biological dissolution of $Ca_3(PO_4)_2$ in low pH medium (Table S3). Conversely, under alkaline conditions, although the initial solubilization efficiency was lower, the solubilization capacity gradually increased during cultivation, ultimately reaching levels comparable to those under neutral conditions. By the end of incubation, the pH values of the culture media across all treatment groups converged, indicating the strain possesses a certain degree of pH self-regulation during growth. Considering both solubilization efficiency and process stability across under different initial pH conditions confirmed pH 7.0 as the optimal condition for phosphate solubilization by strain HRY1.

At the optimal conditions of glucose as carbon source, ammonium sulfate as nitrogen source, and pH 7.0, further optimization of inoculum size was conducted, with results shown in Figure 4d. Strain HRY1 achieved consistently high phosphate solubilization across inoculum sizes of 1% to 8%, with maximum solubilization efficiencies ranging narrowly from 16.27% (8%) to 16.39% (1%). The corresponding soluble phosphorus concentrations were similarly stable, varying between 172.10 (8%) and 174.04 mg L^{-1} (2%) (Table S4). During the early cultivation stage, the 1% inoculum group exhibited lower solubilization efficiency, primarily due to limited initial biomass. In contrast, the 8% inoculum group demonstrated the fastest initiation of phosphate solubilization owing to its higher initial cell density. As cultivation progressed, the solubilization efficiency of the 1% inoculum group increased markedly, eventually reaching levels comparable to groups with higher inoculum sizes. Taking into account both solubilization efficiency and economic feasibility, 1% was determined as the optimal inoculum size for strain HRY1.

Following the optimization of culture conditions (carbon source, nitrogen source, pH, and inoculum size), the influence of initial phosphorus concentration on the phosphate solubilization efficiency of strain HRY1 was further investigated. As shown in Figure 5 and Table S5, under optimized culture conditions, the maximum phosphate solubilization efficiencies and corresponding soluble phosphorus concentrations reached 4.87% (29.25 mg L^{-1}), 15.77% (166.00 mg L^{-1}), and 16.46% (252.15 mg L^{-1}) at initial phosphorus concentrations of 2.5, 5.0, and 15.0 g L^{-1}, respectively. The results also revealed that the maximum phosphate solubilization efficiency reached a plateau when the initial phosphorus concentration surpassed 5.0 g L^{-1}, with no significant differences among the treatments. Conversely, solubilization efficiency declined significantly at concentrations below this

threshold. This implies that a suboptimal $Ca_3(PO_4)_2$ concentration limits the ability of strain HRY1 to fully exert its phosphate-solubilizing capacity.

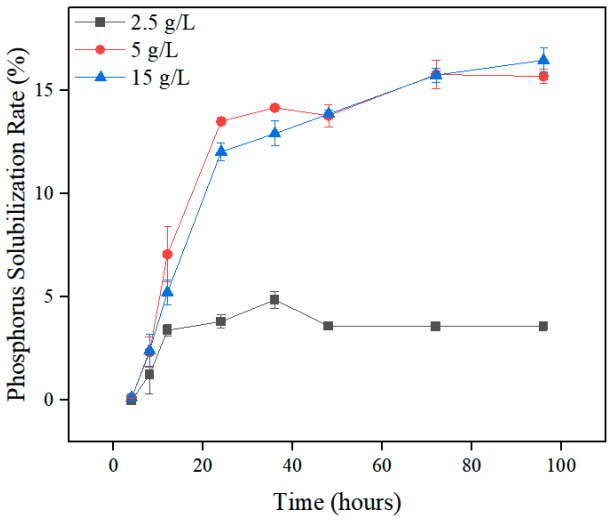


Figure 5. Effect of different $Ca_3(PO_4)_2$ concentrations on the phosphate-solubilizing capacity of strain HRY1.

3.4. Whole-Genome Sequence Analysis of Strain HRY1

3.4.1. Basic Genomic Features

The whole-genome sequencing results of strain HRY1 revealed a total genome length of 4,558,107 bp with a GC content of 50.83%. A total of 4351 protein-coding genes were predicted, with an average length of 915.11 bp. Additionally, 87 tRNA and 22 rRNA genes were identified. Based on these genomic characteristics, a circular genome map of HRY1 was constructed to systematically visualize its genomic architecture and functional features (Figure 6).

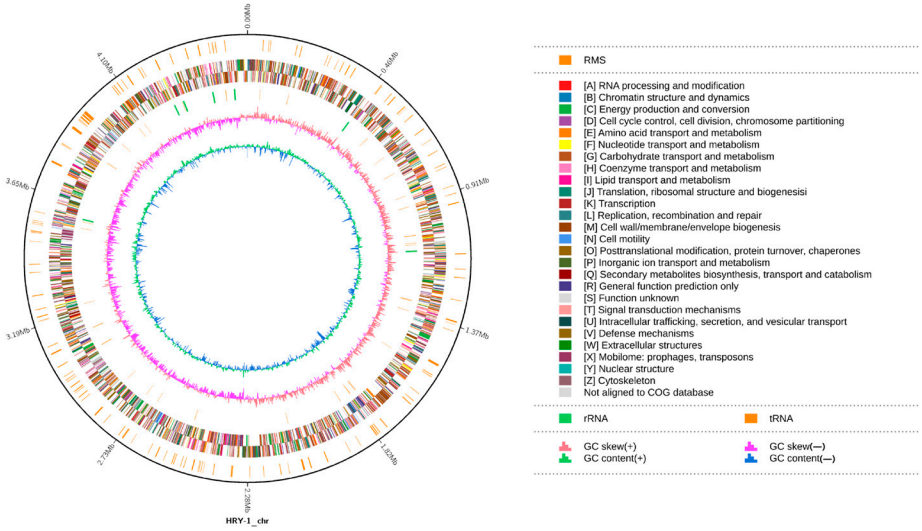


Figure 6. Circular genome map of strain HRY1.

3.4.2. NR Database Annotation

The NR database integrates multiple authoritative sources including GenBank, PDB, SwissProt, PIR, and PRF, enabling systematic revelation of species evolutionary relationships at the protein functional level. By aligning and annotating the predicted protein sequences of strain HRY1 against the NR database, the results are shown in Figure 7. The

annotation results indicate that strain HRY1 shares a homology of 73.21% with proteins from *E. coli*. This finding strongly aligns with the species classification based on 16S rRNA gene sequence analysis, further confirming *E. coli* as the species of HRY1 at the level of protein functional evolution. While methods such as Average Nucleotide Identity (ANI) offer a direct nucleotide-level comparison for species delineation, the NR-based analysis provides valuable insight into conserved biological functions and evolutionary relationships across taxa. Future studies will include ANI calculation to complement these findings.

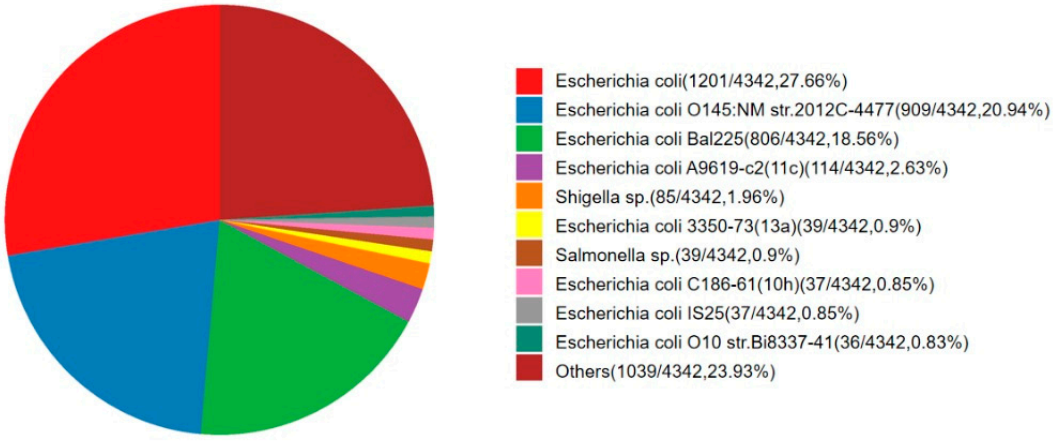


Figure 7. NR annotation taxonomic classification of strain HRY1.

3.4.3. KEGG Database Annotation and Analysis of Genes Related to Phosphorus Metabolism

According to current research, functional genes related to the phosphorus cycle can be primarily categorized into three major classes, encompassing seven functional groups. These include key processes such as phosphorus activation (e.g., phosphate ester mineralization and inorganic phosphate solubilization), phosphorus absorption (e.g., phosphonate transport and inorganic phosphate transport), and phosphorus stress response regulation [11]. To systematically assess the metabolic potential of strain HRY1, its predicted protein sequences was annotated using the KEGG database. KEGG enables the association of genomic genes with systemic functions at cellular, organismal, and ecosystem levels, thereby facilitating systematic annotation of gene functions. The annotation results (Figure 8) revealed that 3855 genes of strain HRY1 were assigned KEGG functional annotations. Among these, the most abundant categories included carbohydrate metabolism (374 genes), membrane transport (276 genes), amino acid metabolism (254 genes), signal transduction (212 genes), metabolism of cofactors and vitamins (201 genes), energy metabolism (194 genes), and nucleotide metabolism (119 genes). These results indicate that HRY1 harbors versatile metabolic repertoire, with particularly prominent functional potential in carbon and nitrogen metabolism, as well as energy metabolism.

Pathway statistics and manual verification of functional genes in the genome of strain HRY1 were performed, with results summarized in Table 1. A total of 16 genes related to inorganic phosphorus solubilization were identified, which could be categorized into three functional classes: organic acid synthesis and phosphorus solubilization-related genes (8 genes: *gcd*, *ack*A, *aro*K, *glt*A, *ilv*H, *gdh*, *pyc*, and *pyk*); phosphorus compound transport-related genes (5 genes: *pit*, *pst*A, *pst*B, *pst*C, and *pst*S); and phosphorus stress response regulatory genes (3 genes: *pho*R, *pho*B, and *pho*U). These results demonstrate that HRY1 possesses a comprehensive genetic toolkit for phosphorus solubilization, uptake, and regulation at the molecular level, providing the genetic basis for its efficient phosphate-solubilizing capacity.

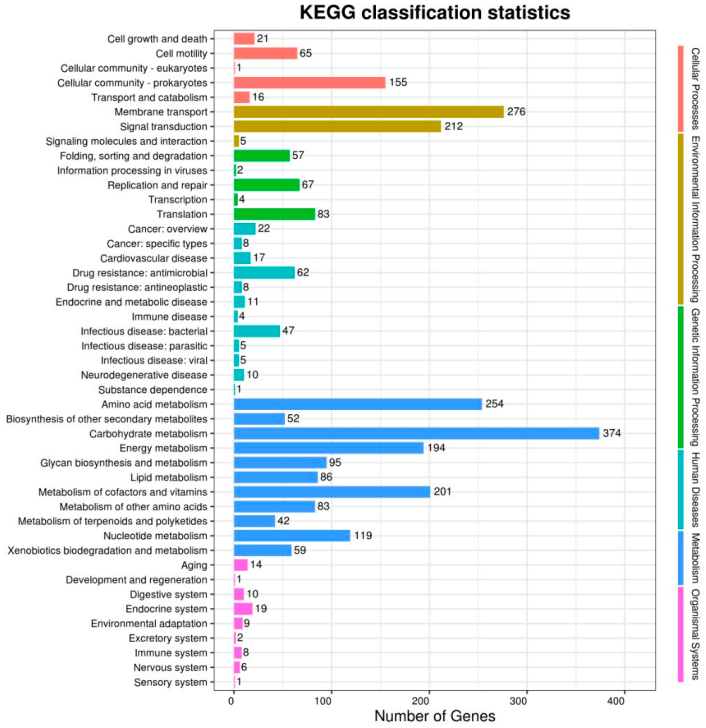


Figure 8. KEGG annotation taxonomic classification of strain HRY1.

Table 1. Genes related to organic acid synthesis and phosphorus metabolism in strain HRY1.

Functional Group	Gene_ID	Gene	KEGG Annotation Function Description
Inorganic phosphorus decomposition	orf03540	*gcd*	quinoprotein glucose dehydrogenase
	orf01360	*ack*A	acetate kinase
	orf00334	*aro*K	shikimate kinase
	orf02944	*glt*A	citrate synthase
	orf03587	*ilv*H	acetolactate synthase I small subunit
	orf00717	*gdh*	glucose 1-dehydrogenase
	orf03437	*pyc*	pyruvate carboxylase
	orf02011	*pyk*	pyruvate kinase
Inorganic phosphate transport	orf00229	*pit*	inorganic phosphate transporter
	orf04331	*pst*A	phosphate transport system permease protein
	orf04332	*pst*B	phosphate transport system ATP-binding protein
	orf04330	*pst*C	phosphate transport system permease protein
	orf04329	*pst*S	phosphate transport system substrate-binding protein
Phosphorus deficiency response regulation	orf03236	*pho*B	phosphate regulon response regulator
	orf03235	*pho*R	phosphate regulon sensor histidine kinase
	orf04333	*pho*U	Negative regulatory proteins of the PhoR/PhoB two-component regulators

Furthermore, to visually represent the arrangement and relative positions of the aforementioned phosphorus metabolism-related genes on the HRY1 chromosome, a gene cluster schematic was generated (Figure 9). In this diagram, the direction of each arrow denotes the transcriptional orientation of the corresponding gene, and the arrow length represents its relative size, collectively offering a clear illustration of the genomic organization and structural architecture of these key functional genes.

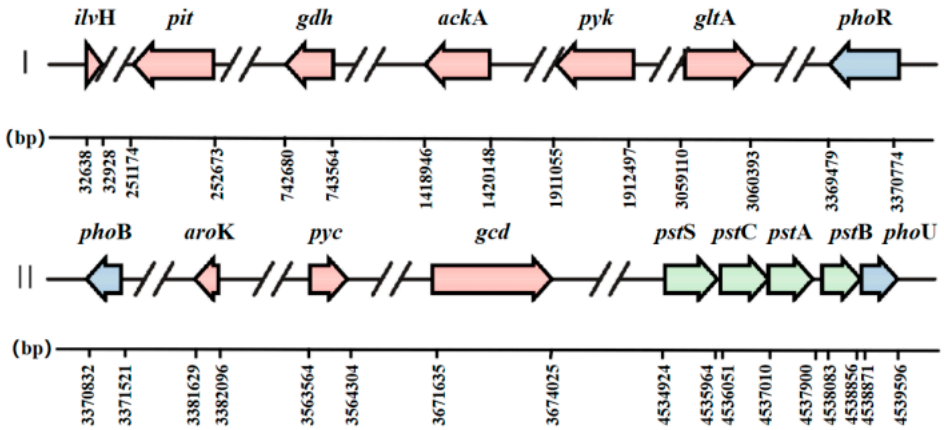


Figure 9. Gene cluster structure of inorganic phosphate solubilization genes. Gene names are labeled above each arrow. Arrow direction indicates transcriptional orientation (right: + strand; left: − strand), arrow length is proportional to gene size, and the numbers below each arrow denote the chromosomal coordinates (in bp).

4. Discussion

Previous studies have demonstrated that strains with phosphorus-solubilizing capabilities are phylogenetically diverse, with representative isolates commonly affiliated with genera such as *Bacillus*, *Pseudomonas*, *Serratia*, *Azotobacter*, *Burkholderia*, *Klebsiella*, and *Pantoea* [12]. In this study, a highly efficient PSB strain, designated HRY1, was successfully isolated and identified as *E. coli*—a species not traditionally regarded as a PSB. Under optimized conditions, HRY1 achieved a tricalcium phosphate dissolution efficiency of approximately 16%, corresponding to a stable solubilized phosphate concentration exceeding 160 mg L^{-1}. The phosphate-solubilizing capacity observed in this study is comparable to or even exceeds that of recently reported phosphate-solubilizing bacterial strains—such as *Acinetobacter soli* AU4 (TCP solubilization: 120.36 mg L^{-1}) and RG6 (112.82 mg L^{-1})—when assessed under the same NBRIP medium system [13]. This finding not only expands the known phylogenetic diversity of phosphate-solubilizing microorganisms but also highlights *E. coli* as a promising candidate for high-efficiency phosphate solubilization, underscoring its potential as a novel microbial resource in this context.

Phosphate-solubilizing efficiency has been shown to vary markedly under different nutritional conditions [14]. As the principal energy source for heterotrophic microorganisms, carbohydrates play a pivotal role in modulating microbial growth, proliferation, and metabolic activity, with distinct carbon sources exerting differential effects depending on their biochemical properties and metabolic accessibility [15]. In the present study, *E. coli* strain HRY1 exhibited maximal phosphate solubilization when glucose was supplied as the sole carbon source. This superior performance likely stems from the organism's preference for readily metabolizable substrates like glucose, whose simple structure and efficient integration into central carbon metabolism supply ample energy and intermediates to drive phosphate solubilization—outperforming other carbon sources tested [16]. Nitrogen availability critically influences microbial physiology and metabolic output [17]. While microorganisms can utilize diverse nitrogen sources—ranging from inorganic forms (e.g., NH_4^+, NO_3^-) to organic compounds (e.g., amino acids, urea)—they typically favor ammonium due to its direct assimilation into central metabolism. In contrast, nitrate requires energy-intensive reduction, and organic nitrogen must be hydrolyzed before uptake, resulting in lower metabolic efficiency [18]. Consistent with this principle, strain HRY1 exhibited significantly higher phosphate-solubilizing activity with NH_4^+–N than with NO_3^-–N. This difference correlates with distinct organic acid secretion profiles: under

NH_4^+–N, HRY1 predominantly produced acetic acid—a potent solubilizer of inorganic phosphorus—whereas NO_3^-–N conditions favored oxalic acid, which displays comparatively weaker solubilization efficacy [19]. This metabolic preference mirrors the canonical "ammonium preference" of *E. coli*, in which energetically efficient nitrogen assimilation supports rapid growth and enhances competitive fitness in nutrient-transforming processes such as phosphate solubilization [20].

Strain HRY1 demonstrated optimal degradation efficiency under neutral pH conditions, a finding consistent with the results reported by Arup Sen et al. [21] for PSB isolated from acidic soils. Furthermore, HRY1 exhibited robust growth across a broad pH range of 6.0–9.0, indicating its considerable environmental adaptability and suggesting potential advantages for application in soil environments with varying pH levels. Inoculum size exerted a limited influence on phosphate solubilization efficiency. When the inoculum exceeded 1%, further increases did not significantly enhance phosphate solubilization—particularly during the later stages of incubation—indicating that the phosphate-solubilizing capacity of HRY1 is primarily associated with its growth-promoting characteristics rather than mere inoculum quantity. This observation aligns with findings of Pereira et al., who reported that lower inoculum levels of phosphate-solubilizing bacteria could, under certain conditions, more effectively promote maize growth [22], suggesting a complex, non-linear relationship between inoculum density and plant-microbe interactions. The phosphate solubilization efficiency of strain HRY1 was significantly influenced by the initial phosphorus concentration. The strain demonstrated enhanced phosphate-solubilizing capacity at higher $Ca_3(PO_4)_2$ concentrations, whereas its solubilization efficiency was markedly suppressed under low-phosphorus conditions. This trend is consistent with existing research conclusions [23]. A high-phosphorus environment may act as a stress signal, activating the expression of phosphate-solubilizing genes such as *pit* (inorganic phosphate transporter) in HRY1, thereby enhancing its ability to dissolve insoluble phosphorus. In contrast, under low-phosphorus conditions, this pathway remains inadequately activated, resulting in limited phosphate solubilization functionality.

It is widely recognized that the primary mechanism by which microorganisms solubilize inorganic phosphorus involves acidolysis [24]. Specifically, PSB produce organic acids (e.g., lactic, malic, succinic acids), which not only decrease the ambient pH but also chelate cations such as Mg^{2+}, Fe^{2+}, and Al^{2+}. This process enhances the bioavailability of phosphorus by releasing it from insoluble complexes, making it accessible for plant uptake. Genomic analysis of HRY1 revealed a total of eight genes involved in the solubilization of inorganic phosphorus and five genes encoding phosphorus compound transporters. Among these, the citrate synthase gene (*glt*A) plays a pivotal role. The *glt*A gene encodes an enzyme that catalyzes the synthesis of citrate from oxaloacetate and acetyl-CoA. The citrate secreted extracellularly effectively promotes the dissolution of insoluble phosphates through acidification and chelation mechanisms [25,26]. Furthermore, the HRY1 strain carries the *aro*K gene, which encodes shikimate kinase—a key enzyme in the shikimate pathway that indirectly enhances shikimate biosynthesis and thereby improves the strain's capacity to solubilize insoluble inorganic phosphorus [27]. Moreover, the *gcd* gene, which encodes glucose dehydrogenase (GDH) for gluconic acid production, was identified in the HRY1 genome [28]. GDH mediates an important acidification mechanism in PSB, and the presence of *gcd* is often used as a molecular marker for inorganic phosphate solubilization potential [29,30]. The *pst* gene cluster, previously reported in other phosphate-solubilizing bacteria such as *Nguyenibacter* sp. L1 [31], was also identified in HRY1 and is pivotal for high-affinity phosphate transport—a process integral to efficient phosphorus solubilization [32]. It should be noted that while our genomic analysis identified a complete set of functional genes, indicating that HRY1 has the potential to dissolve phosphate through

organic acid mediation, this study did not directly measure the secretion levels of specific organic acids (such as gluconic acid and citric acid) or the dynamic changes in culture pH during cultivation. Therefore, the currently proposed phosphate-solubilization mechanism model is mainly based on genomic information and indirect inference from existing literature, and has not yet been directly supported by biochemical evidence. Future studies integrating metabolomics and real-time pH monitoring will be essential to elucidate the dominant phosphate-solubilization pathways in HRY1.

Furthermore, HRY1 possesses the complete set of phosphorus stress response regulatory genes *pho*R, *pho*B, and *pho*U. The PhoR/PhoB two-component system, comprising the transmembrane histidine kinase sensor protein encoded by *pho*R and the cytoplasmic transcriptional response regulator encoded by *pho*B, governs the expression of multiple genes within the Pho regulon [33]. The bacterial phosphorus sensing pathway also requires auxiliary proteins such as the metal-binding protein PhoU encoded by *pho*U. Under conditions of phosphorus scarcity, this Pho regulatory system is activated, coordinating the expression of multiple genes involved in phosphorus uptake and utilization. Consequently, this activation enhances the solubilization of insoluble phosphorus in soil, increasing phosphorus bioavailability and facilitating the strain's adaptation to low-phosphorus environments [34].

Despite these advantageous genetic traits for phosphorus acquisition, the agricultural application of *E. coli* HRY1 warrants careful evaluation. As a highly diverse species, *E. coli* encompasses various ecological groups, including symbiotic, environmentally adapted, and pathogenic types. Prior to developing this strain as a biofertilizer, its biosafety level must be systematically determined in accordance with relevant guidelines and standards. Furthermore, before conducting field trials, it is necessary to comprehensively assess its colonization ability in soil, potential impacts on native microbial community structures, and genetic stability under controlled conditions, so as to scientifically and systematically evaluate its ecological risks. This study provides a theoretical foundation for the exploration and utilization of phosphate-solubilizing microbial resources, but its practical application prospects should be contingent upon thorough biosafety assessments and ecological adaptability verification.

5. Conclusions

This study successfully isolated a highly efficient PSB, identified as *E. coli* HRY1. The strain exhibited consistent and stable phosphate-solubilizing activity, achieving a maximum solubilization efficiency exceeding 16%. Under the conditions tested in this study, strain HRY1 exhibited relatively high phosphate-solubilizing efficiency when cultured with glucose as the carbon source, ammonium sulfate as the nitrogen source, an initial pH of 7.0, an inoculum size of 1%, and a $Ca_3(PO_4)_2$ concentration of 5 g/L. This parameter combination appears to be favorable for enhancing phosphate solubilization by HRY1 within the current experimental system. Genomic analysis revealed that HRY1 harbors 16 genes associated with inorganic phosphorus solubilization and phosphorus metabolism. The primary mechanism contributing to its phosphate-solubilizing capacity involves the regulation of key genes responsible for synthesizing of organic acids, such as citric acid and gluconic acid, which facilitate the dissolution of insoluble phosphorus via acidification and chelation mechanisms. Additionally, HRY1 possesses a complete low-phosphorus stress response system, comprising the PhoR/PhoB two-component regulatory system and auxiliary proteins like PhoU. This comprehensive stress response system endows HRY1 with strong adaptive potential under phosphorus-limited conditions. Overall, our findings highlight the significant potential of *E. coli* HRY1 as a promising biofertilizer candidate for enhancing soil phosphorus availability and promoting plant growth, particularly in phosphorus-deficient environments. Future studies should focus on field trials to vali-

date these results and explore the broader ecological implications of deploying HRY1 in agricultural systems.

Supplementary Materials: The following supporting information can be downloaded at: https://www.mdpi.com/article/10.3390/fermentation12020113/s1, Table S1: Soluble P concentrations under different carbon sources; Table S2: Soluble P concentrations under different nitrogen sources; Table S3: Soluble P concentrations under different pH; Table S4: Soluble P concentrations under different inoculum sizes; Table S5: Soluble P concentrations under different initial phosphorus concentrations.

Author Contributions: Funding acquisition, Y.L.; Project administration, Y.L.; Supervision, Y.L.; Writing—original draft, R.H.; Experiment, R.H. and S.Z.; Writing—review & editing, Y.L. All authors have read and agreed to the published version of the manuscript.

Funding: This study was financially supported by the National Natural Science Foundation of China (No. 52400188).

Data Availability Statement: The data that support the findings of this study are available from the corresponding author upon reasonable request.

Conflicts of Interest: The authors declare that the research was conducted in the absence of any commercial or financial relationships that could be construed as a potential conflict of interest.

References

1. Wang, F.; Deng, M.; Xu, J.; Zhu, X.; Mao, C. Molecular mechanisms of phosphate transport and signaling in higher plants. *Semin. Cell Dev. Biol.* **2018**, *74*, 114–122. [CrossRef]
2. McLaren, T.I.; Smernik, R.J.; McLaughlin, M.J.; Doolette, A.L.; Richardson, A.E.; Frossard, E. The chemical nature of soil organic phosphorus: A critical review and global compilation of quantitative data. *Adv. Agron.* **2020**, *160*, 51–124.
3. Nassef, K.; Sahli, A.; Bouhdid, S.; Mezzoug, N.; Abrini, J.; Khay, E.O. Phosphate solubilizing microorganisms and their use in sustainable agriculture: A review. *Geomicrobiol. J.* **2025**, *42*, 224–243. [CrossRef]
4. Yu, X.; Keitel, C.; Dijkstra, F.A. Global analysis of phosphorus fertilizer use efficiency in cereal crops. *Glob. Food Secur.* **2021**, *29*, 100545. [CrossRef]
5. Joshi, S.; Gangola, S.; Jaggi, V.; Sahgal, M. Functional characterization and molecular fingerprinting of potential phosphate solubilizing bacterial candidates from Shisham rhizosphere. *Sci. Rep.* **2023**, *13*, 7003. [CrossRef] [PubMed]
6. Kalayu, G. Phosphate Solubilizing Microorganisms: Promising Approach as Biofertilizers. *Int. J. Agron.* **2019**, *2019*, 4917256. [CrossRef]
7. Silva, L.I.D.; Pereira, M.C.; Carvalho, A.M.X.D.; Buttrós, V.H.; Pasqual, M.; Dória, J. Phosphorus-solubilizing microorganisms: A key to sustainable agriculture. *Agriculture* **2023**, *13*, 462. [CrossRef]
8. Kumar, S.; Diksha Sindhu, S.S.; Kumar, R. Harnessing phosphate-solubilizing microorganisms for mitigation of nutritional and environmental stresses, and sustainable crop production. *Planta* **2025**, *261*, 95. [CrossRef]
9. Bakki, M.; Banane, B.; Marhane, O.; Esmaeel, Q.; Hatimi, A.; Barka, E.A.; Azim, K.; Bouizgarne, B. Phosphate solubilizing *Pseudomonas and Bacillus* combined with rock phosphates promoting tomato growth and reducing bacterial canker disease. *Front. Microbiol.* **2024**, *15*, 1289466. [CrossRef]
10. Wang, Y.Z.; Jia, L.H.; Tian, G.; Dong, Y.H.; Zhang, X.; Zhou, Z.F.; Luo, X.; Li, Y.; Yao, W. shinyCircos-V2.0: Leveraging the creation of Circos plot with enhanced usability and advanced features. *IMeta* **2023**, *2*, e109. [CrossRef]
11. Siles, J.A.; Starke, R.; Martinovic, T.; Fernandes, M.L.P.; Orgiazzi, A.; Bastida, F. Distribution of phosphorus cycling genes across land uses and microbial taxonomic groups based on metagenome and genome mining. *Soil Biol. Biochem.* **2022**, *174*, 108826. [CrossRef]
12. Ughamba, K.T.; Ndukwe, J.K.; Lidbury, I.D.E.A.; Nnaji, N.D.; Eze, C.N.; Aduba, C.C.; Groenhof, S.; Chukwu, K.O.; Anyanwu, C.U.; Nwaiwu, O.; et al. Trends in the application of phosphate-solubilizing microbes as biofertilizers: Implications for soil improvement. *Soil Syst.* **2025**, *9*, 6. [CrossRef]
13. Berza, B.; Sekar, J.; Vaiyapur, P.; Pagano, M.C.; Assefa, F. Evaluation of inorganic phosphate solubilizing efficiency and multiple plant growth promoting properties of endophytic bacteria isolated from root nodules of *Erythrina brucei*. *BMC Microbiol.* **2022**, *22*, 276. [CrossRef]
14. Li, H.; Chen, S.; Wang, M.; Shi, S.; Zhao, W.; Xiong, G.; Zhou, J.; Qu, J. Phosphate solubilization and plant growth properties are promoted by a lactic acid bacterium in calcareous soil. *Appl. Microbiol. Biotechnol.* **2024**, *108*, 11–14. [CrossRef]

15. Ma, Q.; Yi, J.; Tang, Y.; Geng, Z.; Zhang, C.; Sun, W.; Liu, Z.; Xiong, W.; Wu, H.; Xie, X. Co-utilization of carbon sources in microorganisms for the bioproduction of chemicals. *Biotechnol. Adv.* **2024**, *73*, 108380. [CrossRef]
16. Tiwari, B.; Sindhu, V.; Mishra, A.K.; Singh, S.S. Carbon catabolite repression of methyl parathion degradation in a bacterial isolate characterized as a *Cupriavidus sp.* LMGR1. *Water Air Soil Pollut.* **2020**, *231*, 357. [CrossRef]
17. Deb, S.; Lewicka-Szczebak, D.; Rohe, L. Microbial nitrogen transformations tracked by natural abundance isotope studies and microbiological methods: A review. *Sci. Total Environ.* **2024**, *926*, 172073. [CrossRef] [PubMed]
18. Pan, W.; Zhou, J.; Tang, S.; Wu, L.; Ma, Q.; Marsden, K.A.; Chadwick, D.R.; Jones, D.L. Utilisation and transformation of organic and inorganic nitrogen by soil microorganisms and its regulation by excessive carbon and nitrogen availability. *Biol. Fertil. Soils* **2023**, *59*, 379–389. [CrossRef]
19. Scervino, J.M.; Papinutti, V.L.; Godoy, M.S.; Rodriguez, M.A.; Della Monica, I.; Recchi, M.; Pettinari, M.J. Medium pH, carbon and nitrogen concentrations modulate the phosphate solubilization efficiency of *Penicillium purpurogenum* through organic acid production. *J. Appl. Microbiol.* **2011**, *110*, 1215–1223. [CrossRef]
20. Wang, J.; Yan, D.; Dixon, R.; Wang, Y.P. Deciphering the principles of bacterial nitrogen dietary preferences: A strategy for nutrient containment. *mBio* **2016**, *7*, e00792-16. [CrossRef]
21. Sen, A.; Saha, N.; Sarkar, A.; Poddar, R.; Pramanik, K.; Samanta, A. Assessing the effectiveness of indigenous phosphate-solubilizing bacteria in mitigating phosphorus fixation in acid soils. *3 Biotech* **2024**, *14*, 197. [CrossRef] [PubMed]
22. Pereira, S.I.A.; Sousa, A.S.S.; Felpeto, A.B.; Miguel, A.; Pinto, J.C.; Castro, P.M.L.; Moreira, H. Lower inoculum sizes of phosphorus-solubilizing bacteria benefit maize growth and soil enzyme activity in P-fertilized soils. *Symbiosis* **2025**, *96*, 261–269. [CrossRef]
23. Dai, Z.; Liu, G.; Chen, H.; Chen, C.; Wang, J.; Ai, S.; Wei, D.; Li, D.; Ma, B.; Tang, C.; et al. Long-term nutrient inputs shift soil microbial functional profiles of phosphorus cycling in diverse agroecosystems. *ISME J.* **2020**, *14*, 757–770. [CrossRef]
24. Ahash, S.; Manikandan, K.; Devi, T.S.; Elamathi, S.; Maragatham, S.; Subrahmaniyan, K. Phosphate-solubilizing microorganisms for sustainable phosphorus management in rice. *Rhizosphere* **2025**, *34*, 101096. [CrossRef]
25. Adhikari, P.; Pandey, A. Phosphate solubilization potential of endophytic fungi isolated from *Taxus wallichiana* Zucc. roots. *Rhizosphere* **2019**, *9*, 2–9. [CrossRef]
26. McKay Fletcher, D.M.; Ruiz, S.; Dias, T.; Petroselli, C.; Roose, T. Linking root structure to functionality: The impact of root system architecture on citrate-enhanced phosphate uptake. *New Phytol.* **2020**, *227*, 376–391. [CrossRef]
27. Guo, D.J.; Yang, G.R.; Singh, P.; Wang, J.J.; Lan, X.M.; Singh, R.K.; Guo, J.; Dong, Y.D.; Li, D.P.; Yang, B. Comprehensive analysis of the physiological and molecular responses of phosphate-solubilizing bacterium *Burkholderia gladioli* DJB4-8 in promoting maize growth. *Front. Plant Sci.* **2025**, *16*, 1611674. [CrossRef]
28. An, R.; Moe, L.A. Regulation of pyrroloquinoline quinone-dependent glucose dehydrogenase activity in the model rhizosphere-dwelling bacterium *Pseudomonas putida* KT2440. *Appl. Environ. Microbiol.* **2016**, *82*, 4955–4964. [CrossRef]
29. Pang, F.; Li, Q.; Solanki, M.K.; Wang, Z.; Xing, Y.X.; Dong, D.F. Soil phosphorus transformation and plant uptake driven by phosphate-solubilizing microorganisms. *Front. Microbiol.* **2024**, *15*, 1383813. [CrossRef]
30. Peng, Y.; Huang, Z.; Bian, F.; Wu, Z.; Zhong, Z.; Zhang, X. Characteristics of microbial phosphorus cycling in Phyllostachys praecox forest soils supplemented with the phosphate-solubilizing bacterium *Pseudomonas* sp. OP1 revealed by metagenomics. *J. Environ. Manag.* **2025**, *394*, 127363. [CrossRef]
31. Li, X.L.; Lv, X.Y.; Ji, J.B.; Wang, W.D.; Wang, J.; Wang, C.; He, H.B.; Ben, A.L.; Liu, T.L. Complete genome sequence of *Nguyenibacter* sp. L1, a phosphate solubilizing bacterium isolated from Lespedeza bicolor rhizosphere. *Front. Microbiol.* **2023**, *14*, 1257442. [CrossRef] [PubMed]
32. Cui, S.; Wang, Z.; Kong, L.; Zhang, M.; Xu, H.; Xiao, P.; Tao, Y. Dynamics of microbial communities and functional genes under the interactions between phosphorus inactivation agents and phosphorus-solubilizing bacteria in sediments. *J. Water Process Eng.* **2025**, *77*, 108395. [CrossRef]
33. Oliverio, A.M.; Bissett, A.; McGuire, K.; Saltonstall, K.; Turner, B.L.; Fierer, N. The role of hosphorus limitation in shaping soil bacterial communities and their metabolic capabilities. *mBio* **2020**, *11*, e01718-20. [CrossRef] [PubMed]
34. Khan, A.A.; Chen, Y.; Asghar, R.M.A.; Azeem, I.; Shah, T.; Cao, W.; Zhang, D.; Gao, Y. P-solubilising bacteria and P-cycling genes drive soil P transformation during green manure decomposition. *Agric. Ecosyst. Environ.* **2025**, *394*, 109875. [CrossRef]

Disclaimer/Publisher's Note: The statements, opinions and data contained in all publications are solely those of the individual author(s) and contributor(s) and not of MDPI and/or the editor(s). MDPI and/or the editor(s) disclaim responsibility for any injury to people or property resulting from any ideas, methods, instructions or products referred to in the content.